Eur. Phys. J. Appl. Phys. **46**, 20403 (2009)
DOI: 10.1051/epjap/2009038

THE EUROPEAN PHYSICAL JOURNAL APPLIED PHYSICS

Regular Article

Evaluation of organic sub-monolayers by X-ray based measurements under gracing incident conditions

O. Werzer[1,a], B. Stadlober[2], A. Haase[2], H.-G. Flesch[1], and R. Resel[1]

[1] Institute of Solid State Physics, Graz University of Technology, Graz, Austria
[2] Institute of Nanostructured Materials and Photonics, Joanneum Research Forschungsgesellschaft mbH, Weiz, Austria

Received: 16 September 2008 / Received in final form: 20 November 2008 / Accepted: 20 January 2009
Published online: 27 March 2009 –

Abstract. The structural investigations of model organic systems like pentacene on silicon oxide in the monolayer regime is very important for the basic understanding of initial nucleation process together with the electronic performance of transistor devices. A method for the evaluation of the island formation and layer closing of the first monolayer is introduced. The method is based on specular X-ray reflectivity and diffuse scattering and reveal integral information on the coverage together with the size and separation of pentacene islands. The results are in good agreement with AFM investigation that encourages the use of this type of investigation in in-situ experiments.

PACS. 61.05.cc Theories of X-ray diffraction and scattering – 61.05.cm X-ray reflectometry (surfaces, interfaces, films) – 61.43.Hv Fractals; macroscopic aggregates (including diffusion-limited aggregates) – 68.35.bm Polymers, organics

1 Introduction

Small molecules like pentacene, sexithipohene or sexiphenyl are widely used in organic electronic research. The high reproducibility of thin films by vacuum deposition of the molecules together with good electronic performance make them perfect materials for studying the basic properties of organic electronic devices. The variation of process parameters [1,2] together with the variations of substrates [3,4] gives the possibility to study the structural properties of an organic thin film from the monolayer to the bulk. The charge transport within an organic transistor device is mainly influenced by the first few layers [5,6]. Therefore the structure within the first layers is extremely important for the basic understanding of electronic device performance.

Defined growth conditions provide the possibility to produce high quality and reproducible thin films that can be used to evaluate the nucleation within the mono and multi layer regime. The investigations of the island formation that is often observed within the growth of organic thin films prepared from small molecules [4,7,8] can be performed with atomic force microscopy [9]. Information on the island size, island shape and island distribution are easily accessible. Although the morphological information can be extracted from AFM measurements the crystallographic information are not accessible. For this purpose X-ray based techniques can be used to identify the real structure within the film (e.g. grain size). Of particular interest is the number of grains within one island since this influences directly the charge transport through a transistor device [10]. The evaluation of the crystallographic properties during the growth process is therefore of interest. Hence fluctuation in the thin film formation occur for several samples, in-situ experiments are necessary to be able to evaluate the evolution of the islands formation with increasing coverage. Since combined AFM and X-ray measurements are hard to realize X-ray based methods for the nucleation behavior of the film, i.e. island size, shape and separation has to be used.

Ex-situ specular X-ray reflectivity (s-XRR) and diffuse or off-specular X-ray scattering (o-XRR) are used within this work to investigate a model organic system in the submonolayer regime. The results are combined with AFM investigations to verify the obtained parameters. The results encourage the use of this methods within X-ray based in-situ growth experiment to achieve additional information on the nucleation behavior of organic thin films.

2 Experimental

Pentacene films were grown onto silicon wafers with 196 nm thick thermal oxide. The substrate is used as-delivered without any further cleaning procedure. The vacuum during deposition was 2×10^{-6} mbar. The substrate temperature was 337 K and the growth rate below 1 nm/min monitored by a microbalance. The deposited

[a] e-mail: o.werzer@gmx.at

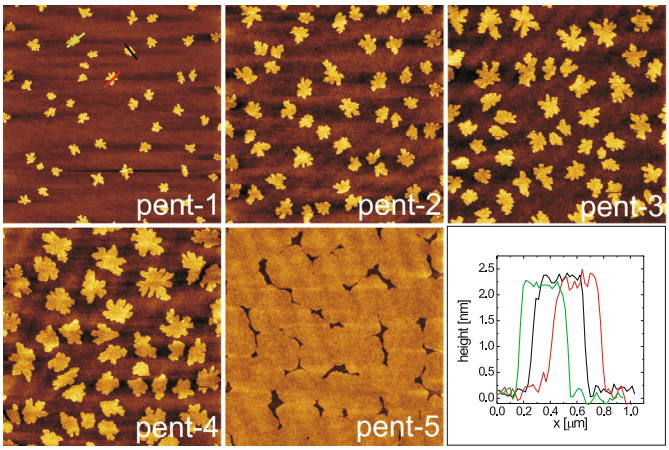

Fig. 1. (Color online) 10×10 μm^2 tapping mode AFM height images of pentacene film with different coverages starting from 7% (pent-1) to 95% (pent-5). The AFM cross sections from three different pentacene islands of sample pent-1 are shown at bottom right.

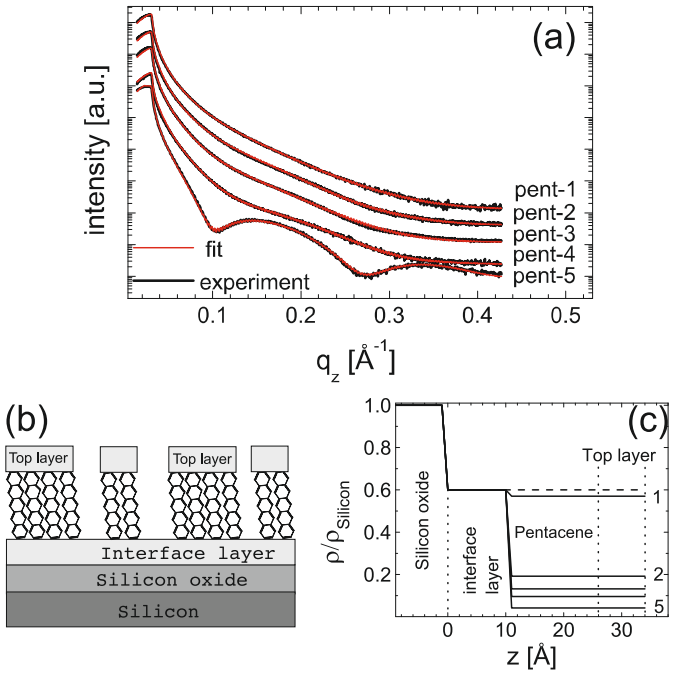

Fig. 2. (Color online) Specular X-ray reflectivity measurements (a) for pentacene films with different coverages ranging from 7% (top curve) to 95% (bottom curve). The curves are shifted for clarity. A scheme of the model for the simulation is shown (b). Normalized electron density distribution obtained from the fit for the different samples (c). The dashed line indicates the electron density of pentacene from structure solution.

films were investigated with a Dimension 3100 (Digital Instruments, Inc.) atomic force microscope (AFM) in tapping mode. Specular and off-specular X-ray measurements are performed with a Bruker D8-Discover diffractometer. The radiation is provided by a copper sealed tube with a wavelength of 0.154 nm and is monochromatized with a secondary side graphite monochromator. The resolution was adjusted with the divergence slit, anti-scatter slit and receiving slit. All slits were set to 0.1 mm. Additional two Soller slits are introduced. The integration time was adjusted for the different scans to optimize the counting statistics.

3 Results

Pentacene thin films with different coverages are investigated by AFM measurements. The scans are depicted in Figure 1. The images show the typical nucleation behavior of pentacene thin films on isotropic surfaces. The island diameters for the different samples ranges from 150 nm to 2000 nm. The height of an island is about 2.5 nm that is slightly larger than a single monolayer of pentacene in the thin film phase. The separation of the islands is about 1.5 μm.

Specular XRR measurements were performed to evaluate the electron density perpendicular to the sample surface, whereby the electron density is a direct measure of the coverage of the layers. s-XRR measurements were performed on the samples with different coverages (compare Fig. 2a). The organic layer produced a shallow oscillation for the lowest coverage (compare pent-1 Fig. 2). Films with higher coverages produced more pronounced oscillations whereby the highest coverage (pent-5) reveals the most pronounced oscillations. The fitting of the specular reflectivity data was performed with the dynamical Parratt formalism [11] and the Nevot-Croce model [12].

The parameters of the experimental setup together with the substrate parameters were determined prior and were hold constant during the fitting procedure. The model depicted in the Figure 2b was developed to achieve reasonable fitting results with the organic layer. The assumption of the fit was that the film grows in the thin film phase, i.e. the pentacene molecules are in a standing configuration with the long molecular axis nearly perpendicular to the substrate. According to literature the height of the pentacene was set fixed with 1.54 nm during the fit procedure. Additionally, an interface layer had to be introduced between the first pentacene islands and the substrate. On top of the standing molecules another layer was required to be able to fit the experimental data. The coverage is calculated via comparison of the electron density of the film with the electron density of the crystal structure of the thin film phase [13]. The obtained electron density distributions of the fit are plotted in Figure 2c and the relevant parameters are listed in Table 1.

Specular scans (q_z-scans at $q_x = 0$) do not offer a possibility to get information on the lateral distribution of the islands since it is only a measure of the electron density along the surface normal. Lateral information can be achieved by q_x-scans or by combined $q_x q_z$ scans. In the small angular region rocking curves are sufficient to achieve a q_x-scan at $q_z \sim$ constant. Several rocking curves at different q_z values are measured for sample pent-4. The results are depicted in Figure 3. The scans reveal a

Table 1. Characteristic parameters of the pentacene thin films and the fitting results of the specular reflectivity measurements: nominal thickness determined by microbalance (*nom. t*), coverage determined by AFM (cov_{AFM}), thickness of the interface layer (d_{int}) and coverage determined by XRR (cov_{XRR}).

no.	*nom. t* (nm)	cov_{afm} (%)	d_{int} (nm)	cov_{xrr} (%)
pent-1	0.3	7	0.71	8
pent-2	0.6	16	0.75	12
pent-3	0.9	22	0.72	17
pent-4	1.2	32	0.81	39
pent-5	2.4	95	0.87	94

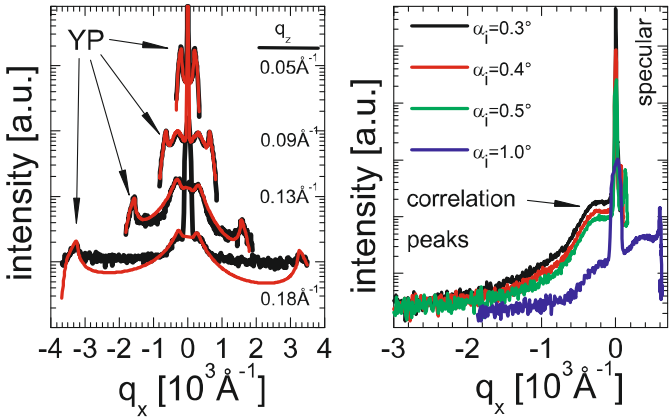

Fig. 3. (Color online) Rocking curve at different q_z values for sample pent-4 (left). Black lines denotes experimental data, red line the fit and YP the position of Yoneda peak. Curves are shifted for clarity. Detector scans vs. in-plane component of the scattering vector for different incident angles performed on sample pent-4 (right).

symmetric intensity distribution with respect to the strong specular peak ($q_x = 0$). The curves are terminated on both sides by the Yoneda peaks [14]. For the rocking scans at higher q_z values additional peak (shoulder) like features occur at $q_x = \pm 2.8 \times 10^{-4}$ Å^{-1}. Since the peaks are located at the same position for the different q_z-values the underlying reason is a reciprocal space property of the sample. The occurrence of the peaks is caused by the island form, size and lateral distribution. A description of the simulation of the rocking curve measurements is given in the next section.

Similar information about the islands can be obtained by detector scans at grazing incident conditions. Detector scans at different incident angles were taken (Fig. 3b). The curves show the strong specular peak at $q_x = 0$. Next to the specular peak on the right hand side the Yoneda belonging to the transmission function of the exiting beam is obtained. At $q_x = \pm 2.8 \times 10^{-4}$ Å^{-1} a shoulder can be identified that is the same as shown in the rocking curves above but measured in different directions in reciprocal space.

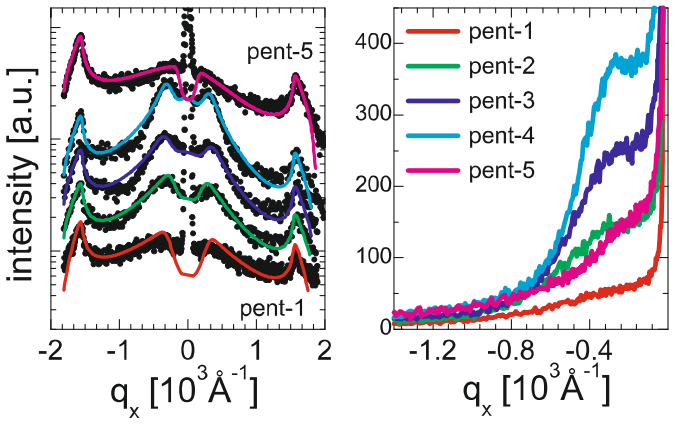

Fig. 4. (Color online) Rocking curves measurements (dots) and fit results (full lines) for different coverages measured at $q_z = 0.129$ Å^{-1} (left). Curves are shifted for clarity. Intensity in counts vs. in-plane component of the scattering vector from detectorscans with incident angle of 0.25 deg (right).

Table 2. Lateral parameters from AFM and rocking curve fits. Mean island size (R_{AFM}) and separation (d_{AFM}) evaluated with AFM. Mean island size (R_{o-XRR}) and mean island separation (d_{o-XRR}) evaluated by X-ray diffraction. (*) denotes the valleys within the pentacene film.

no.	R_{AFM} (nm)	d_{AFM} (μm)	R_{o-XRR} (nm)	d_{o-XRR} (μm)
pent-1	147	1.46	210	1.25
pent-2	315	1.51	310	1.35
pent-3	485	1.41	469	1.12
pent-4	754	1.22	700	1.36
pent-5*	142*	1.71*	160*	2.16*

Rocking scans performed at $q_z = 0.129$ Å^{-1} and detector scans taken at an incident angle of 0.25 deg for the various samples are shown in Figure 4. All scans look comparable to the scans of sample pent-4 whereby the intensity of the shoulder increases with increasing coverage starting from 7% coverage (pent-1) up to a coverage of 32% (pent-4). The nearly full covered film (pent-5) shows a damped shoulder with an amplitude between pent-1 and pent-2. The theoretical description of the rocking curve results is given in the next section. In Table 2 the extracted informations of rocking curve fits are listed.

4 Theoretical description of rocking curves

Several approaches for the calculation of the diffuse scattered intensity from geometrical object can be used [25–27]. The model used here is based on [28] modified with the effective layer approximation whereby here only the rocking curves are considered. For simplicity the specular peak is not considered whereby the width of the taken out region is determined by the rocking curve measurement of the pure substrate.

The diffuse scattering (non-specular) is described by the differential cross section in the Born approximation by:

$$\frac{d\sigma}{d\Omega_{diff}} \sim |F(q)|^2 \cdot S(q) \cdot |t(\alpha_i)|^2 |t(\alpha_f)|^2 \quad (1)$$

whereby q is the scattering vector, $F(q)$ denotes the form factor of a pentacene island and $S(q)$ denotes the lateral mass center separation of the islands. $t(\alpha_{i,f})$ are the transmission function of the incoming and exiting beam, respectively. The form factor of an island is approximated with a cylinder shape [22]. Taking into account a certain size distribution of the cylinders the form factor reads as:

$$F_p(q_x) = \sum_k p(R_k)\pi R_k^2 \frac{J_1(q_x, R_k)}{q_x R_k} \quad (2)$$

where J_1 is the Bessel function of order one and R is the radius of the cylinder. $p(R_k)$ denotes the statistical variation of the island size whereby the gamma distribution was chosen that writes as:

$$p(R_k) = \phi^M / \Gamma(M) \exp(-\phi R_k) R_k^{M-1} \quad (3)$$

with ϕ and M are the parameters of the gamma distribution. The structure factor is a function of the island distribution. Choosing the paracrystal model for the spatial distribution of the islands the structure factor writes as:

$$S = \frac{1 - D^2(q_x)}{1 - 2D(q_x)\cos(q_x d) + D^2(q_x)} \quad (4)$$

with $D = \exp(-q_x^2\sigma^2)$ and $\overline{d}$ as the mean separation of the island mass centers. σ denotes the variation of $\overline{d}$. With the theoretical model introduced here the rocking curves can be fitted by least-square fitting routine. The extracted mean island size and island separation of the fitting results are summarized in Table 2. For comparison the same quantities determined from AFM images are given aswell.

5 Discussion

The AFM images reveal a reproducible single layer growth of pentacene films from the sub-monolayer regime to the closed monolayer. The reproducibility is proven since the variation of the mass-center distances of the islands is small for all samples (pent-1 to pent-5). This can be seen on the one hand by the AFM pictures and on the other hand by the rocking curve measurements. The nucleation density is in good agreement with literature values of pentacene grown on silicon oxidized substrates [3].

The s-XRR results reveal the presence of an additional layer within the mono-layer pentacene films. The assumption of standing molecules on top of an interface layer is in excellent agreement with literature [3]. Since the specular reflectivity is not chemically sensitive, it is not possible to clarify the chemical nature of the interface layer. Literature gives indications of a water layer present between the pentacene and the silicon oxide [15]. A detailed surface study of water adsorption and desorption on silicon oxide surfaces for different temperature and different pressures reveals the presence of a water layer wit 9 Å thickness as very unlikely [16]. A wetting layer consisting of lying molecules of pentacene like it is observed on pure silicon surface [17] would be more likely and would also explain the same growth behavior for different substrates [4]. NEXAFS experiments performed on similar samples shows the possibility of pentacene molecules orientated lying edge-on with the long molecular axis parallel to the substrate surface [18]. Optical experiments on a similar system (sexithiophene on silicon oxide) reveal the presence of lying molecules and standing molecules on the same sample as well [19]. Anyway, the nature of this interface layer can not be clarified with the methods in use and is not aim of this work.

Concerning the results from the rocking curve measurements it can be concluded that the introduced model can describe the experimental data. The reasonable match between the results from AFM and the X-ray experiments show some deviations. On the one hand an improvement of the simulation can be obtained by taking into account the fractal character of the islands. On the other hand the experimental setup needs to be improved to reduce broadening due to the finite coherence [20]. From [21] a upper limit for our experimental setup of the coherence length of 15 μm can be estimated. Therefore it can be concluded that the patterns produced from the islands are the partially coherent sum of the different islands. The limited flux from the sealed tube also limits the ability to measure rocking curves at higher q_z values. This can be seen by the rocking curves measured at $q_z = 1.8$ Å where the intensity between the Yoneda peak and the correlation peak is at the background level. In addition the values obtained for pent-5 are much too small, but occur due to the model that does not take into account the refractive indices of the organic layer. Therefore the obtained parameters for pent-5 represents the holes within the film and not the islands, however it is in good agreement with the AFM results.

Even if the results are not accurate enough to get more detailed information than from the AFM measurements it shows an excellent opportunity to get additional information within in-situ experiments. For coverages below 50% the amplitude of the peak belonging to the correlation increases with increasing coverage. For higher coverages the peak is getting more and more depressed until the first layer is fully covered. It is expected that the increasing coverage in the second layer produces a similar oscillating pattern. Since the layer-by-layer growth of organic films often disappears due to rapid roughening [23] the use of the anti-Bragg point scattering evaluation will be favorable to evaluate the films during an in-situ film growth [24]. Hence the anti-Bragg points are connected to the slit interference function of the crystal it is only possible to evaluate the film if more than two mono layers are present.

A detailed in-situ study of the island size and distribution like shown here together with grazing incident

diffraction would reveal more information on the initial growth behavior of organic thin films within the first monolayer. Especially the possibility to obtain further information on the number of grains within one island.

6 Summary and conclusion

Model organic thin films from pentacene in the sub-monolayer regime are prepared onto thermally oxidized silicon wafers. The AFM investigation of the films reveal the typical island formation of pentacene for the isotropic surface of silicon oxide. The measurements of the specular X-ray reflectivity and off-specular scans by means of rocking curve and detector scans reveal excellent agreements with the values determined by AFM. The models worked out can identify the coverage, the island size and the island separation. These informations are very useful especially for in-situ experiments to evaluate the growth behavior of organic thin films in the first monolayer.

The work was supported by the Austrian Nanoinitiative within the project cluster ISOTEC, subproject N705 NANO and by the Austrian Science Foundation (FWF) within the NFN project: Interface controlled and functionalized organic films.

References

1. I. Yagi, K. Tsukagoshia, Y. Aoyagi, Thin Solid Films **467**, 168 (2004)
2. Y. Wu, T. Toccoli, N. Koch, E. Iacob, A. Pallaoro, P. Rudolf, S. Iannotta, Phys. Rev. Let. **98**, 076601 (2007)
3. R. Ruiz, B. Nickel, N. Koch, L.C. Feldman, R.F. Haglund, A. Kahn, G. Scoles, Phys. Rev. B **67**, 125406 (2003)
4. B. Stadlober, U. Haas, H. Maresch, A. Haase, Phys. Rev. B **74**, 165302 (2006)
5. F. Dinelli, M. Murgia, P. Levy, M. Cavallini, F. Biscarini, D.M. de Leeuw, Phys. Rev. Lett. **92**, 116802 (2004)
6. B.N. Park, S. Seo, P.G. Evans, J. Phys. D: Appl. Phys. **40**, 3506 (2007)
7. F.J. Meyer zu Heringdorf, M.C. Reuter, R.M. Tromp, Nature **412**, 517 (2001)
8. M. Brinkmann, D. Pratontep, C. Contal, Surf. Sci. **600**, 4712 (2006)
9. R. Ruiz, B. Nickel, N. Koch, L.C. Feldman, R.F. Haglund, A. Kahn, F. Family, G. Scoles, Phys. Rev. Lett. **91**, 136102 (2003)
10. K. Puntambekar, J. Dong, G. Haugstad, C.D. Frisbie, Adv. Funct. Mater. **16**, 879 (2006)
11. L.G. Parratt, Phys. Rev. **95**, 359 (1954)
12. L. Nevot, P. Croce, Rev. Phys. Appl. **15**, 761 (1980)
13. D. Nabok, P. Puschnig, O. Werzer, R. Resel, D.-M. Smilgies, C. Amborsch-Draxl, Phys. Rev. B **76**, 235322 (2007)
14. Y. Yoneda, Phys. Rev. **131**, 2010 (1963)
15. A.C. Mayer, R. Ruiz, R.L. Headrick, A. Kazimirov, G.G. Malliaras, Org. Electron. **5**, 257 (2005)
16. O. Sneh, M.A. Cameron, S.M. George, Surf. Sci. **364**, 61 (1996)
17. F.-J. Meyer zu Heringdorf, J. Phys.: Condens. Matter **20**, 184007 (2008)
18. G. Yoshikawa, T. Miyadera, R. Onoki, K. Ueno, I. Nakai, S. Entani, S. Ikeda, D. Guo, M. Kiguchi, H. Kondoh, T. Ohta, K. Saiki, Surf. Sci. **600**, 2518 (2006)
19. M.A. Loi, E. Da Como, F. Dinelli, M. Murgia, R. Zamboni, F. Biscarini, M. Muccini, Nat. Mat. **81**, 4 (2005)
20. R. Stoemmer, U. Pietsch, J. Phys. D: Appl. Phys. **29**, 3161 (1996)
21. U. Pietsch, V. Holy, T. Baumbach, *High Resolution X-ray Scattering*, 2nd edn. (Springer-Verlag, New York, 2004), p. 46
22. R. Lazzari, J. Appl. Cryst. **35**, 406 (2002)
23. S. Kowarik, A. Gerlach, W. Leitenberger, J. Hu, G. Witte, C. Woell, U. Pietsch, F. Schreiber, Thin Solid Films **515**, 5606 (2007)
24. S. Kowarik, A. Gerlach, F. Schreiber, J. Phys.: Condens. Matter **20**, 184005 (2008)
25. F. Leroy, R. Lazzari, G. Renaud, Surf. Sci. **601**, 1915 (2007)
26. V. Holy, A.A. Darhuber, J. Stangl, G. Bauer, J. Nuetzel, G. Abstreiter, Semicond. Sci. Technol. **13**, 590 (1998)
27. P.R. Pukite, C.S. Lent, P.I. Cohen, Surf. Sci. **161**, 39 (1985)
28. G. Vignaud, A. Gibaud, J. Wang, S.K. Sinha, J. Daillant, G. Grubel, Y. Gallot, J. Phys.: Condens. Matter **9**, L125 (1997)